PHYSICAL REVIEW D **67**, 033005 (2003)

Bounds on the tau and muon neutrino vector and axial vector charge radius

Martin Hirsch
Instituto de Física Corpuscular, CSIC/Universitat de València, Edificio Institutos de Paterna, Apt 22085 E-46071 València, Spain

Enrico Nardi
INFN Laboratori Nazionali di Frascati, C. P. 13, I00044 Frascati, Italy
and Departamento de Física, Universidad de Antioquia A.A. 1226 Medellín, Colombia

Diego Restrepo
Departamento de Física, Universidad de Antioquia A.A. 1226 Medellín, Colombia

(Received 22 October 2002; published 27 February 2003)

A Majorana neutrino is characterized by just one flavor diagonal electromagnetic form factor, the anapole moment, which in the static limit corresponds to the axial vector charge radius $\langle r_A^2\rangle$. Experimental information on this quantity is scarce, especially in the case of the tau neutrino. We present a comprehensive analysis of the available data on the single photon production process $e^+e^-\to\nu\bar{\nu}\gamma$ off Z resonance, and we discuss the constraints that these measurements can set on $\langle r_A^2\rangle$ for the τ neutrino. We also derive limits for the Dirac case, when the presence of a vector charge radius $\langle r_V^2\rangle$ is allowed. Finally, we comment on additional experimental data on ν_μ scattering from the NuTeV, E734, CCFR, and CHARM-II Collaborations, and estimate the limits implied for $\langle r_A^2\rangle$ and $\langle r_V^2\rangle$ for the muon neutrino.

DOI: 10.1103/PhysRevD.67.033005 PACS number(s): 13.15.+g, 13.40.Gp, 14.60.St

I. INTRODUCTION

Experimental evidence for neutrino oscillations [1–4] implies that neutrinos are the first elementary particles whose properties cannot be fully described within the standard model (SM). This hints at the possibility that other properties of these intriguing particles might substantially deviate from the predictions of the SM, and is presently motivating vigorous efforts, on both theoretical and experimental sides, to understand in more depth the detailed properties of neutrinos and of their interactions. In particular, the electromagnetic properties of the neutrinos can play important roles in a wide variety of domains such as cosmology [5] and astrophysics [6,7], and can also provide a viable explanation for the observed depletion of the electron neutrino flux from the Sun [8–13].

The electromagnetic interaction of Dirac neutrinos is described in terms of four form factors. The matrix element of the electromagnetic current between an initial neutrino state ν_i with momentum p_i and a final state ν_j with momentum p_j reads [14,15]

$$\langle \nu_j^D(p_j)|J_\mu^{\rm EM}|\nu_i^D(p_i)\rangle = i\bar{u}_j\Gamma_\mu^D(q^2)u_i,$$

$$\Gamma_\mu^D(q^2) = (q^2\gamma_\mu - q_\mu \not{q})[V^D(q^2) - A^D(q^2)\gamma_5] + i\sigma_{\mu\nu}q^\nu[M^D(q^2) + E^D(q^2)\gamma_5], \qquad (1.1)$$

where $q=p_j-p_i$, and the (ij) indices denoting the relevant elements of the form factor matrices have been left implicit. In the $i=j$ diagonal case, M^D and E^D are called the magnetic and electric form factors, which in the limit $q^2=0$ define, respectively, the neutrino magnetic moment $\mu = M^D(0)$ and the (CP violating) electric dipole moment $\epsilon = E^D(0)$. The reduced Dirac form factor $V^D(q^2)$ and the neutrino anapole form factor $A^D(q^2)$ do not couple the neutrinos to on-shell photons. For $i=j$ and in the $q^2=0$ limit they are related to the vector and axial vector charge radii $\langle r_V^2\rangle$ and $\langle r_A^2\rangle$ through[1]

$$\langle r_V^2\rangle = -6V^D(0), \quad \langle r_A^2\rangle = -6A^D(0). \qquad (1.2)$$

In the following, even when $q^2\neq 0$ we will keep referring to the reduced Dirac form factor and to the anapole form factor as the vector and axial vector charge radii. A long standing controversy about the possibility of consistently defining gauge invariant, physical, and process independent vector and axial vector charge radii [16] has been recently settled [17–20]. The controversy was related to the general problem of defining improved one-loop Born amplitudes in SU(2) $\times$U(1) for four-fermion processes, like, for example, $e^+e^-\to f\bar{f}$. If one tries to take into account one-loop vertex corrections by defining improved effective couplings, one finds that gauge invariance cannot be preserved unless, together with other one-loop contributions, W box diagrams are also added to the amplitude. However, box diagrams connect initial state fermions to the final states, and thus depend on the specific process. Due to the absence of neutrino-photon coupling at the tree level, the problem is even more acute when trying to define the charge radius as a physical, process independent property, intrinsic to neutrinos. In [17] it was realized that for neutrino scattering off right handed po-

[1]The vector charge radius is defined as the second moment of the spatial charge distribution $\langle r_V^2\rangle = \int r^2\rho_V(r)d\vec{r}$ where $\rho_V(r)$ is the Fourier transform of the full Dirac form factor $q^2V^D(q^2)$. The axial vector charge radius can be defined in a completely similar way.

larized fermions, the W box diagrams are absent to begin with, and thus no ambiguity arises. This suggested a way to derive a unique decomposition of loop contributions that separately respects gauge invariance, and from which a process independent charge radius could be defined as an intrinsic property of the neutrino. Furthermore, in [18,20] it was argued that the charge radius so defined is a physical observable, namely, its value can be extracted, at least in principle, from experiments.

For Majorana neutrinos, in the nondiagonal case ($\nu_j^M \neq \nu_i^M$) and in the limit of CP invariance the electromagnetic interaction is described by just two form factors [14]. If the initial and final Majorana neutrinos involved in the process have the same CP parity, only $E_{ji}^M(q^2)$ and $A_{ji}^M(q^2)$ are nonvanishing, while if the CP parity is opposite, the electromagnetic interaction is described by $M_{ji}^M(q^2)$ and $V_{ji}^M(q^2)$. Finally, in the diagonal Majorana case $\nu_j^M = \nu_i^M$ the only surviving form factor is the anapole moment $A^M(q^2)$. As discussed in [21], this last result can be inferred from the requirement that the final state of the two identical fermions in $\gamma \to \nu^M \overline{\nu^M}$ be antisymmetric, and therefore it holds regardless of the assumption of CP invariance.

In the SM the neutrino electromagnetic form factors have extremely small values [22]. Because of the left-handed nature of the weak interactions, the numerical values of the vector and axial vector charge radii coincide, and for the different ν_e, ν_μ, and ν_τ flavors they fall within the range [17] $\langle r_{V,A}^2 \rangle \approx (1-4)\times 10^{-33}$ cm^2.[2] However, since neutrinos do show properties that are not accounted for by the SM, it could well be that their electromagnetic interactions also deviate substantially from the SM expectations.

In general, the strongest limits on the neutrino electromagnetic form factors come from astrophysical and cosmological considerations. For example, the neutrino magnetic moments can be constrained from considerations of stellar energy losses through plasma photon decay $\gamma \to \nu\overline{\nu}$ [23], from the nonobservation of anomalous energy loss in the Supernova 1987A neutrino burst as would have resulted from the rapid emission of superweakly interacting right-handed neutrinos [23], and from big bang nucleosynthesis arguments. In this last case, the agreement between the measurements of primordial helium abundance and the standard nucleosynthesis calculations imply that, for example, spin flipping Dirac magnetic moment interactions should be weak enough not to populate right-handed neutrinos degrees of freedom at the time when the neutron-to-proton ratio freezes out [5].

Since the charge radii do not couple neutrinos to on-shell photons, the corresponding interactions are not relevant for stellar evolution arguments. However, in the Dirac case, right-handed neutrinos can still be produced through, e.g., $e^+e^- \to \nu_R \overline{\nu}_R$, and therefore the constraints from the Supernova 1987A as well as from nucleosynthesis do apply. They yield, respectively [24], $|\langle r^2 \rangle| \lesssim 2\times 10^{-33}$ cm^2 and [25] $|\langle r^2 \rangle| \lesssim 7\times 10^{-33}$ cm^2.[3]

However, if neutrinos are Majorana particles, they do not have light right-handed partners, and the previous constraints do not apply. In this case, in particular for the τ neutrino, an anapole moment corresponding to an interaction even stronger than electroweak could be allowed. In the early Universe such an interaction could keep ν_τ in thermal equilibrium long enough to experience a substantial reheating from $e^+e^- \to \nu_\tau \overline{\nu}_\tau$ annihilation. We have investigated to what extent this reheating could affect the Universe expansion rate and change the predictions for primordial helium abundance. As we will discuss in Sec. II, we have found that even an interaction one order of magnitude stronger than electroweak would hardly affect helium abundance at an observable level.

We conclude that constraints on the Majorana neutrino axial charge radius can be obtained only from terrestrial experiments. The present laboratory limits for the electron neutrino are [26] $-5.5\times 10^{-32} \lesssim \langle r_A^2(\nu_e) \rangle \lesssim 9.8\times 10^{-32}$ cm^2 [67][4] Of course, in the Dirac case these limits apply to the sum $\langle r_V^2 \rangle + \langle r_A^2 \rangle$ as well. Limits for the muon neutrino have been derived from ν_μ scattering experiments [27,28]. They are about one order of magnitude stronger than for the electron neutrinos, and will be discussed in Sec. IV. Because of the fact that intense ν_τ beams are not available in laboratories, to date no direct limits on $\langle r_A^2(\nu_\tau) \rangle$ have been reported by experimental collaborations. However, under the assumption that a significant fraction of the neutrinos from the sun converts into ν_τ, by using the SNO and Super-Kamiokande observations the limit $|\langle r_A^2(\nu_\tau) \rangle| \lesssim 2\times 10^{-31}$ cm^2 has been derived [29]. A limit on the ν_τ vector charge radius (Dirac case) was derived by analyzing KEK TRISTAN data on the single photon production process $e^+e^- \to \nu\overline{\nu}\gamma$ [30]. The same data can be used to constrain also the anapole moment for a Majorana ν_τ, and therefore we have included TRISTAN measurements in our set of constraints.

In the next section we will briefly analyze the possibility of deriving constraints on the Majorana neutrino axial charge radius from nucleosynthesis. In Sec. III we will study the bounds on the tau neutrino charge radius implied by the TRISTAN and CERN e^+e^- LEP experimental results. In Sec. IV we will discuss the constraints on the muon neutrino charge radius from the NuTeV, CHARM-II, CCFR, and BNL E734 experiments. They result in the following 90% C.L. limits:

$$-8.2\times 10^{-32}\ \text{cm}^2 \lesssim \langle r_A^2(\nu_\tau) \rangle \lesssim 9.9\times 10^{-32}\ \text{cm}^2, \tag{1.3}$$

[2]These values are obtained in the $q^2=0$ limit, and decrease with increasing energies with a logarithmic behavior.

[3]In the SM with right-handed neutrinos ν_R cannot be produced through the charge radius couplings, since the vector and axial vector contributions exactly cancel. Therefore, the quoted limits implicitly assume that, because of new physics contributions, one of the two form factors dominates and no cancellations occur.

[4]These limits are twice the values published in [26] since we are using a convention for $\langle r_{V,A}^2 \rangle$ that differs by a factor of 2.

$$-5.2\times10^{-33}\ \text{cm}^2 \leqslant \langle r_A^2(\nu_\mu)\rangle \leqslant 6.8\times10^{-33}\ \text{cm}^2. \tag{1.4}$$

For $\langle r_A^2(\nu_e)\rangle$ we could not find new experimental results that would imply better constraints than the existing ones [26]. We just mention that the Bugey nuclear reactor data from the detector module closest to the neutrino source (15 m) [31] should imply independent limits of the same order of magnitude as the existing ones.

II. NUCLEOSYNTHESIS

In this section we study the possible impact on the primordial helium abundance Y of an axial charge radius large enough to keep a Majorana ν_τ in thermal contact with the plasma down to temperatures $T<1$ MeV. In this case the neutrinos would get reheated by e^+e^- annihilation, and this would affect the Universe expansion rate. To give an example, if one neutrino species is maintained in thermal equilibrium until e^+e^- annihilation is completed ($T\ll m_e$) this would affect the expansion as $\Delta\nu=1-(4/11)^{4/3}\simeq0.74$ additional neutrinos.

The amount of helium produced in the early Universe is determined by the value of the neutron to proton ratio n/p at the time when the $ne^+\leftrightarrow p\bar{\nu}$ and $n\nu\leftrightarrow pe^-$ electroweak reactions freeze out. This occurs approximately at a temperature $T_{fo}\approx0.7$ MeV [32,33]. Apart from the effect of neutron decay, virtually all the surviving neutrons end up in ^{4}He nuclei. Assuming no anomalous contributions to the electron-neutrino reactions, the freeze-out temperature can only be affected by changes in the Universe expansion rate, which is controlled by the number of relativistic degrees of freedom and by their temperature. If tau neutrinos have only standard interactions, at the time of the freeze-out they are completely decoupled from the thermal plasma. However, an anomalous contribution to the process $e^+e^-\leftrightarrow\nu_\tau\bar{\nu}_\tau$ would allow the ν_τ to share part of the entropy released in e^+e^- annihilation. The maximum effect is achieved assuming that the new interaction is able to keep the ν_τ thermalized down to T_{fo}. The required strength of the new interaction can be estimated by equating the rate for an anomalously fast $e^+e^-\leftrightarrow\nu_\tau\bar{\nu}_\tau$ process $\Gamma_{\nu_\tau}=\langle\sigma v\rangle n_e$ to the Universe expansion rate $\Gamma_U=(8\pi\rho/3m_P^2)^{1/2}$. In the previous formulas $\langle\sigma v\rangle$ is the thermally averaged cross section times the relative velocity, $n_e\approx0.365T^3$ is the number density of electrons, $\rho\approx1.66g_*^{1/2}(T^2/m_P)$ is the Universe energy density with $g_*\approx10.75$ the number of relativistic degrees of freedom, and m_P is the Plank mass. The thermally averaged cross section can be written as $\langle\sigma v\rangle\simeq\kappa G_{\nu_\tau}^2T^2$ where $G_{\nu_\tau}\approx(2\pi^2\alpha/3)\langle r_A^2\rangle$ parametrizes the strength of the interaction and is assumed to be sensibly larger than the Fermi constant G_F, and $\kappa\approx0.2$ has been introduced to allow direct comparison with the SM rate $\langle\sigma v\rangle^{SM}\simeq0.2\,G_F^2T^2$ [32]. By setting $\Gamma_{\nu_\tau}=\Gamma_U$ at $T=T_{fo}$, we obtain $G_{\nu_\tau}\approx13\times10^{-5}$ GeV^{-2}. Therefore, to keep the ν_τ thermalized until the ratio n/p freezes out, an interaction about ten times stronger than electroweak is needed.

However, even in the presence of such a large interaction, helium abundance would only be mildly affected. This is because at $T\approx0.7$ MeV e^+e^- annihilation is still not very efficient, and the photon temperature is only slightly above the temperature of thermally decoupled neutrinos: $(T_\gamma-T_\nu)/T_\gamma\approx1.5\%$ [32]. This induces a change in the primordial helium abundance $\Delta Y\approx+0.04(\Delta T_{\nu_\tau}/T_\nu)$ which is below one part in 1000. This effect could possibly be at the level of the present theoretical precision [34] the present observational accuracy, for which the errors are of the order of 1% [35].

III. LIMITS ON ν_τ VECTOR AND AXIAL VECTOR CHARGE RADII

Limits on $\langle r_V^2\rangle$ and $\langle r_A^2\rangle$ for ν_τ can be set using experimental data on single photon production through the process $e^+e^-\to\bar{\nu}\nu\gamma$. In the following we will analyze the data from TRISTAN and the off-resonance data from LEP. These data have been collected over a large energy range, from 58 GeV up to 207 GeV. Given that form factors run with the energy, we will present separate results for the data collected below Z resonance (TRISTAN), for the data between Z resonance and the threshold for W^+W^- production (LEP-1.5), and finally for the data above W^+W^- production (LEP-2). Due to the much larger statistics collected at high energy, a combined fit of all the data does not give any sizable improvement with respect to the LEP-2 limits, which therefore represent our strongest bounds.

The SM cross section for the process $e^+e^-\to\nu\bar{\nu}\gamma$ is given by [36]

$$\frac{d\sigma_{\nu\nu\gamma}}{dxdy}=\frac{2\alpha/\pi}{x(1-y^2)}\left[\left(1-\frac{x}{2}\right)^2+\frac{x^2y^2}{4}\right]\{N_\nu\sigma_s(s',g_V,g_A)+\sigma_{st}(s')+\sigma_t(s')\} \tag{3.1}$$

where σ_s corresponds to the lowest order s channel Z boson exchange with $N_\nu=3$ the number of neutrinos that couple to the Z boson. For later convenience in σ_s we have explicitly shown the dependence on the electron couplings $g_V=-1/2+2\sin^2\theta_W$ and $g_A=-1/2$, where θ_W is the weak mixing angle. The additional two terms σ_{st} and σ_t in Eq. (3.1) correspond respectively to Z-W interference and to t channel W boson exchange in ν_e production. The kinematic variables are the scaled photon momentum $x=E_\gamma/E_{\text{beam}}$ with $E_{\text{beam}}=\sqrt{s}/2$, the reduced center of mass energy $s'=s(1-x)$, and the cosine of the angle between the photon momentum and the incident beam direction $y=\cos\theta_\gamma$. The expressions for the lowest order cross sections appearing in Eq. (3.1) read

$$\sigma_s(s)=\frac{sG_F^2}{6\pi}\frac{\frac{1}{2}(g_V^2+g_A^2)M_Z^4}{(M_Z^2-s)^2+M_Z^2\Gamma_Z^2}, \tag{3.2}$$

$$\sigma_{st}(s)=\frac{sG_F^2}{6\pi}\frac{(g_V+g_A)(M_Z^2-s)M_Z^2}{(M_Z^2-s)^2+M_Z^2\Gamma_Z^2}, \tag{3.3}$$

$$\sigma_t(s) = \frac{sG_F^2}{6\pi}, \tag{3.4}$$

where G_F is the Fermi constant, α the fine structure constant, and M_Z and Γ_Z the mass and width of the Z boson. A few comments are in order. Equation (3.1) was first derived in [36]. It holds at relatively low energies where W exchange in the t channel can be legitimately approximated as a contact interaction. This amounts to neglecting the momentum transfer in the W propagator, and to dropping the W-γ interaction, so that photons are emitted only from the electron lines. While this approximation is sufficiently good at TRISTAN energies, to analyze the LEP data collected above Z resonance some improvements have to be introduced. We will use an improved approximation where finite distance effects are taken into account in the W propagator; however, we will still work in the limit of vanishing W-γ interactions. While strictly speaking the amplitude with the photon attached only to the electron legs is not gauge invariant, the necessary contribution for completing the gauge invariant amplitude is of higher order in a leading log approximation [37], and for our analysis can be safely neglected. Finite distance W exchange effects can be taken into account in the previous expressions through the replacement

$$\sigma_{st}(s) \to \sigma_{st}(s) \cdot F_{st}\left(\frac{s}{M_W^2}\right), \tag{3.5}$$

$$\sigma_t(s) \to \sigma_t(s) \cdot F_t\left(\frac{s}{M_W^2}\right), \tag{3.6}$$

where M_W is the W boson mass, and

$$F_{st}(z) = \frac{3}{z^3}\left[(1+z)^2\log(1+z) - z\left(1+\frac{3}{2}z\right)\right], \tag{3.7}$$

$$F_t(z) = \frac{3}{z^3}[-2(1+z)\log(1+z) + z(2+z)]. \tag{3.8}$$

The contact interaction approximation is recovered in the limit $z \to 0$ for which $F_{st,t}(z) \to 1$.

An anomalous interaction due to nonvanishing ν_τ axial and axial vector charge radii can be directly included in Eq. (3.1) by redefining the Z boson exchange term in the following way:

$$N_\nu \sigma_s(s', g_V, g_A) \to (N_\nu - 1)\sigma_s(s', g_V, g_A) + \sigma_s(s', g_V^*(s'), g_A), \tag{3.9}$$

where

$$g_V^*(s') = g_V - \left[1 - \frac{s'}{M_Z^2}\right]\delta, \tag{3.10}$$

$$\delta = \frac{\sqrt{2}\pi\alpha}{3G_F}[\langle r_V^2\rangle + \langle r_A^2\rangle]. \tag{3.11}$$

The substitution $g_V \to g_V^*$ in Eq. (3.9) takes into account the new photon exchange diagram for production of left-handed ν_τ. In the Dirac case, s channel production of right-handed ν_τ through photon exchange must also be taken into account. This yields a new contribution that adds incoherently to the cross section, and that can be included by adding inside the angular brackets in Eq. (3.1) the term

$$\sigma_R(s') = \frac{s'G_F^2}{6\pi}(\delta')^2, \tag{3.12}$$

$$\delta' = \frac{\sqrt{2}\pi\alpha}{3G_F}[\langle r_V^2\rangle - \langle r_A^2\rangle]. \tag{3.13}$$

In the SM $\langle r_V^2\rangle = \langle r_A^2\rangle$ and therefore there is no production of ν_R through these couplings. For a Majorana neutrino $\delta' = 0$ and $\langle r_V^2\rangle = 0$, and thus the limits on anomalous contributions to the process $e^+e^- \to \nu\bar{\nu}\gamma$ translate into direct constraints on the axial charge radius $\langle r_A^2(\nu_\tau)\rangle$. Note that including anomalous contributions just for the ν_τ is justified by the fact that for ν_e and ν_μ the existing limits are generally stronger than what can be derived from the process under consideration.

A. Limits from TRISTAN

The three TRISTAN experiments AMY [38], TOPAZ [39], and VENUS [40] have searched for single photon production in e^+e^- annihilation at a c.m. energy of approximately $\sqrt{s} = 58$ GeV. Anomalous contributions to the cross section for $e^+e^- \to \nu\bar{\nu}\gamma$ would have been signaled by an excess of events in their measurements. Limits on the tau neutrino charge radius from the TRISTAN data have already been derived in [30]. In the present analysis, we include also the neutrino axial charge radius, and we give an alternative statistical treatment based on a χ^2 analysis and on the measured cross sections, rather than on the number of events observed combined with Poisson statistics as given in [30]. This puts the TRISTAN constraints on a comparable statistical basis with the LEP results discussed in the next section.

TRISTAN data are collected in Table I. The number of single photons observed, including the SM backgrounds, was six for AMY, five for TOPAZ, and eight for VENUS. The numbers listed in the $N_{\rm obs}$ column in Table I are the background subtracted events, which correspond to the measured cross sections $\sigma^{\rm meas}$ given in the fourth column. We have found that our expressions for the cross section (3.1)–(3.8) tend to overestimate the Monte Carlo results quoted by the three collaborations. This might be due to additional specific experimental cuts in addition to the ones quoted in the last two columns in Table I . In any case, the disagreements with the Monte Carlo results remain well below the experimental errors, and therefore we simply consider it as an additional theoretical uncertainty that we add in quadrature. In constructing the χ^2 function, we use conservatively as experimental errors the upper figures of the three measurements. This is justified by the fact that the γ-Z interference term arising from new physics is always subdominant with respect

TABLE I. Summary of the TRISTAN data: The center of mass energy and luminosity are given in the second and third columns. The background subtracted experimental cross sections and the Monte Carlo expectations quoted by the three collaborations are given, respectively, in columns four and five (in femtobarns), while the number of observed events after background subtraction is listed in column six. ϵ is the efficiency of the cuts in percent units. The last two columns collect the kinematic cuts, with $x=E_\gamma/E_{\rm beam}$, $x_T=x\sin\theta_\gamma$ with θ_γ the angle between the photon momentum and the beam direction, and $y=\cos\theta_\gamma$.

	$\sqrt{s}$ (GeV)	$\mathcal{L}$(pb^{-1})	$\sigma^{\rm meas}$ (fb)	$\sigma^{\rm MC}$ (fb)	$N_{\rm obs}$	ϵ(%)	$E_\gamma/E_{\rm beam}$	$\lvert y\rvert$
		55	29^{+25}_{-18}	34		44	$x\geqslant 0.175$	
		91	for	34		64	$x\geqslant 0.175$	
AMY [38]	57.8				$4.2^{+3.7a}_{-2.6}$			$\leqslant 0.7$
		56	($x\geqslant 0.125$	49		58	$x\geqslant 0.125$	
		99	$\lvert y\rvert\leqslant 0.7$)	49		57	$x\geqslant 0.125$	
TOPAZ [39]	58	213	37^{+58}_{-19}	54	$2.2^{+3.4b}_{-1.1}$	27.3	$x\geqslant 0.14$	$\leqslant 0.8$
							$x_T\geqslant 0.12$	
VENUS [40]	58	164.1	$42.0^{+45.3}_{-30.2}$	36.4	$3.9^{+4.2c}_{-2.8}$	57	$x_T\geqslant 0.13$	$\leqslant 0.64$

[a]AMY observes six events in the four runs listed above (respectively 0, 2, 2, 2) with an estimated background of 1.7 ± 0.3 events. The quoted value for $N_{\rm obs}$ has been derived from their background subtracted cross section.

[b]TOPAZ observes five events, and expects $2.5^{+1.5}_{-0.6}$ from background. $N_{\rm obs}$ has been derived from their background subtracted cross section.

[c]VENUS observes eight events and expects $4.1^{+2.4}_{-1.7}$ from background. They quote $3.9^{+4.2}_{-2.8}$ background subtracted $\overline{\nu\nu}\gamma$ events, which correspond to the cross section given in the fourth column.

to the square of the anomalous photon exchange diagram, and therefore new physics contributions would always increase the cross section.

For a Majorana ν_τ ($\delta'=0$ and $\langle r_V^2\rangle=0$) the TRISTAN data imply the following 90% C.L.

$$-3.7\times 10^{-31}\ \text{cm}^2\leqslant\langle r_A^2(\nu_\tau)\rangle\leqslant 3.1\times 10^{-31}\ \text{cm}^2. \tag{3.14}$$

For the Dirac case, the associated production of right-handed states through σ_R in Eq. (3.12) allows us to constrain independently the vector and axial vector charge radius. The 90% C.L. are

$$-2.1\times 10^{-31}\ \text{cm}^2\leqslant\langle r_{V,A}^2(\nu_\tau)\rangle\leqslant 1.8\times 10^{-31}\ \text{cm}^2. \tag{3.15}$$

As we have already mentioned, strictly speaking the constraints just derived cannot be directly compared with the LEP constraints analyzed below, since the two experiments are proving neutrino form factors at different energy scales. Of course, since our limits are meaningful only to the extent that they are interpreted as constraints on physics beyond the SM, it is not possible to make a sound guess at the form of the scaling of the form factors with the energy, which is determined by the details of the underlying new physics. However, if we assume a logarithmic reduction of the form factors with increasing energy as is the case in the SM, than we would expect a moderate reduction of about ≈ 0.65 when scaling from TRISTAN to LEP-1.5 energies, and an additional reduction of about ≈ 0.75 from LEP-1.5 up to LEP-2 measurements at 200 GeV.

B. Limits from LEP

Limits on $\langle r_V^2\rangle$ and $\langle r_A^2\rangle$ can be derived from the observation of single photon production at LEP in a completely similar way. We stress that, contrary to magnetic moment interactions that get enhanced at low energies with respect to electroweak interactions, the interaction corresponding to a charge radius scales with energy roughly in the same way as the electroweak interactions, and therefore searches for possible effects at high energy are not at a disadvantage with respect to low energy experiments. It is for this reason that LEP data above the Z resonance are able to set the best constraints on the vector and axial vector charge radii for the τ neutrino.

All LEP experiments have published high statistics data for the process $e^+e^-\to\nu\overline{\nu}\gamma$ for c.m. energies close to the Z pole; however, due to the dominance of resonant Z boson exchange, these data are not useful to constrain anomalous neutrino couplings to s channel off-shell photons. Therefore, in the following we will analyze LEP data on single photon production collected above Z resonance, in the energy range 130 GeV–207 GeV. We divide the data into two sets: LEP-1.5 data collected below the W^+W^- production threshold are collected in Table II, while LEP-2 data, collected above the W^+W^- threshold and spanning the energy range 161–207 GeV are collected in Table III.

1. LEP-1.5

The ALEPH [41], DELPHI [42], and OPAL [43–45] Collaborations have published data for single photon production at c.m. energies of 130 GeV and 136 GeV. During the fall 1995 runs ALEPH [41] and DELPHI [42] accumulated about 6 pb^{-1} of data for each experiment, observing, respectively,

TABLE II. Summary of the ALEPH, DELPHI, and OPAL data collected the below W^+W^- production threshold. ALEPH [41] and OPAL [44,45] present separate results for two different energies, while DELPHI [42] combines together the data collected at 130 and 136 GeV. DELPHI presents separate data for two different detector components: the high density projection chamber (HPC) covering large polar angles, and the forward electromagnetic calorimeter (FEMC) covering the forward regions. The kinematic cuts applied are given in columns eight and nine. Wherever a double error is listed, the first is statistical and the second is systematic.

LEP-1.5	$\sqrt{s}$ (GeV)	$\mathcal{L}$,(pb^{-1})	$\sigma^{\rm meas}$ (pb)	$\sigma^{\rm MC}$ (pb)	$N_{\rm obs}$	ϵ(%)	E_γ (GeV)	$\lvert y\rvert$
ALEPH	130	2.9	$9.6\pm2.0\pm0.3$	10.7 ± 0.2	23	85		
							$\geqslant 10$	$\leqslant 0.95$
[41]	136	2.9	$7.2\pm1.7\pm0.2$	9.1 ± 0.2	17	85		
DELPHI								
HPC [42]	$\langle 133\rangle$	5.83	$7.9\pm1.9\pm0.7$	—	20	53 [a]	$\geqslant 2$	$\leqslant 0.70$
FEMC [42]	$\langle 133\rangle$	5.83	$6.0\pm1.9\pm0.6$	—	17	43 [a]	$\geqslant 10$	0.83-0.98
OPAL	130	2.30	$10.0\pm2.3\pm0.4$	13.48 ± 0.22 [b]	19	81.6	$x_T>0.05$	$\leqslant 0.82$
							or	
[44]	136	2.59	$16.3\pm2.8\pm0.7$	11.30 ± 0.20 [b]	34	79.7	$x_T>0.1$	$\leqslant 0.966$
	130	2.35	$11.6\pm2.5\pm0.4$	14.26 ± 0.06 [b]	21	77.0		
[45]							$x_T>0.05$	$\leqslant 0.966$
	136	3.37	$14.9\pm2.4\pm0.5$	$11.95\pm0.07^\dagger$	39	77.5		

[a]Estimated from the inferred experimental cross sections and measured numbers of events.
[b]Calculated from the expected number of events as predicted by the KORALZ event generator.

40 and 37 events. In the same runs OPAL [43,44] collected a little less than 5 pb^{-1}, observing 53 events. In addition, OPAL published data also for the 1997 runs (at the same energies) [45], collecting an integrated luminosity of 5.7 pb^{-1} and observing 60 events.

ALEPH reports two values for the cross sections at 130 GeV and 136 GeV, each based on 2.9 pb^{-1} of statistics. They also quote the results of a Monte Carlo calculation of the SM cross section, whcich is in good agreement with the experimental numbers (and with our estimates). DELPHI combined together the statistics of both the 130 GeV and 136 GeV runs, however, they present separate results for two different detector components: the high density Projection Chamber (HPC) covering large polar angles, and the forward electromagnetic calorimeter (FEMC) covering small polar angles. Since DELPHI does not quote any Monte Carlo result we assign a bona fide 5% theoretical error for our cross section estimates. OPAL published two sets of data. The data recorded in the 1995 runs [43] were reanalyzed in [44], and correspond to 2.30 pb^{-1} collected at 130 GeV, and to 2.59 pb^{-1} collected at 136 GeV. In the 1997 runs [45] 2.35 pb^{-1} were collected at 130 GeV, and 3.37 pb^{-1} at 136 GeV. With a total integrated luminosity of about 28 pb^{-1} LEP-1.5 implies the following 90% C.l.

$$-5.9\times10^{-31}\ \text{cm}^2\leqslant\langle r_A^2(\nu_\tau)\rangle\leqslant 6.6\times10^{-31}\ \text{cm}^2 \tag{3.16}$$

for the axial vector charge radius of a Majorana ν_τ, and

$$-3.5\times10^{-31}\ \text{cm}^2\leqslant\langle r_{V,A}^2(\nu_\tau)\rangle\leqslant 3.7\times10^{-31}\ \text{cm}^2 \tag{3.17}$$

for the Dirac case. Let us note that, in spite of the much larger statistics, the limits from LEP-1.5 (3.16) and (3.17) are roughly a factor of 2 worse than the limits from TRISTAN in Eqs. (3.14) and (3.15). The main reason for this is that at LEP-1.5 energies initial state radiation tends to bring the effective c.m. energy of the collision s' close to the Z resonance, thus enhancing Z exchange with respect to the new photon exchange diagram.

2. LEP-2

Above the threshold for W^+W^- production the four LEP experiments collected altogether about 1.6 nb^{-1} of data. The corresponding 24 data points are collected in Table III. ALEPH [46–48] published data for ten different c.m. energies, ranging from 161 GeV up to 209 GeV. Data collected between 203.0 GeV and 205.5 GeV were combined together (they appear in the table as the 205 GeV entry) and the same was done for the data collected between 205.5 GeV and 209.0 GeV that are quoted as the 207 GeV entry. DELPHI [49] published data collected at 183 GeV and 189 GeV, and gives separate results for the three major electromagnetic calorimeters, the HPC, the FEMC and the small angle tile calorimeter (STIC) that covers the very forward regions, between 2° and 10° and 170° and 178°. In three papers [50–52] the L3 Collaboration reported the results obtained at 161 GeV, 172 GeV, 183 GeV, and 189 GeV. While for most data points the agreement between our SM computation of the cross sections and the Monte Carlo results is at the level of 5% or better, we find that the L3 Monte Carlo results are up to 20% larger than our numbers, and this disagreement is encountered for all four L3 data points. While we have not been able to track the reasons for this discrepancy, we have verified that the effects on our final results are negligible. OPAL published data for four different c.m. energies [44,45,53]. For the data presented in [44,45] we have esti-

TABLE III. Summary of the ALEPH, DELPHI, L3, and OPAL experimental data, collected above W^+W^- production threshold. The notation is the same as in Table II. Wherever a double error is listed, the first is statistical and the second is systematic.

LEP-2	$\sqrt{s}$ (GeV)	$\mathcal{L}(\mathrm{pb}^{-1})$	σ^{meas} (pb)	σ^{MC} (pb)	$\mathrm{N}_{\mathrm{obs}}$	$\epsilon(\%)$	E_γ (GeV)	$\lvert y\rvert$
ALEPH	161	11.1	$5.3\pm0.8\pm0.2$	5.81 ± 0.03	41	70		
							$x_T\geqslant0.075$	$\leqslant0.95$
[46]	172	10.6	$4.7\pm0.8\pm0.2$	4.85 ± 0.04	36	72		
[47]	183	58.5	$4.32\pm0.31\pm0.13$	4.15 ± 0.03	195	77	$x_T\geqslant0.075$	$\leqslant0.95$
	189	173.6	$3.43\pm0.16\pm0.06$	3.48 ± 0.05	484			
	192	28.9	$3.47\pm0.39\pm0.06$	3.23 ± 0.05	81			
	196	79.9	$3.03\pm0.22\pm0.06$	3.26 ± 0.05	197			
[48]	200	87.0	$3.23\pm0.21\pm0.06$	3.12 ± 0.05	231	81.5	$x_T\geqslant0.075$	$\leqslant0.95$
	202	44.4	$2.99\pm0.29\pm0.05$	3.07 ± 0.05	110			
	205	79.5	$2.84\pm0.21\pm0.05$	2.93 ± 0.05	182			
	207	134.3	$2.67\pm0.16\pm0.05$	2.80 ± 0.05	292			
DELPHI								
[49]								
	183	50.2	$1.85\pm0.25\pm0.15$	2.04	54	58 [a]		
HPC							$x\geqslant0.06$	$\leqslant0.70$
	189	154.7	$1.80\pm0.15\pm0.14$	1.97	146	51 [a]		
	183	49.2	$2.33\pm0.31\pm0.18$	2.08	65	54 [a]	$x\geqslant0.2$	$\geqslant0.85$
FEMC								
	189	157.7	$1.89\pm0.16\pm0.15$	1.94	155	50 [a]	$x\leqslant0.9$	$\leqslant0.98$
	183	51.4	$1.27\pm0.25\pm0.11$	1.50	32	— [b]	$x\geqslant0.3$	$\geqslant0.990$
STIC								
	189	157.3	$1.41\pm0.15\pm0.13$	1.42	94	— [b]	$x\leqslant0.9$	$\leqslant0.998$
L3	161	10.7	$6.75\pm0.91\pm0.18$	6.26 ± 0.12	57	80.5	$\geqslant10$	$\leqslant0.73$
							and	
[50]	172	10.2	$6.12\pm0.89\pm0.14$	5.61 ± 0.10	49	80.7	$E_T\geqslant6$	0.80–0.97
[51]	183	55.3	$5.36\pm0.39\pm0.10$	5.62 ± 0.10	195	65.4	$\geqslant5$	$\leqslant0.73$
							and	
[52]	189	176.4	$5.25\pm0.22\pm0.07$	5.29 ± 0.06	572	60.8	$E_T\geqslant5$	0.81–0.97
OPAL	161	9.89	$5.3\pm0.8\pm0.2$	6.49 ± 0.08 [c]	40	75.2	$x_T>0.05$	$\leqslant0.82$
							or	
[44]	172	10.28	$5.5\pm0.8\pm0.2$	5.53 ± 0.08 [c]	45	77.9	$x_T>0.1$	$\leqslant0.966$
[45]	183	54.5	$4.71\pm0.34\pm0.16$	4.98 ± 0.02 [c]	191	74.2	$x_T>0.05$	$\leqslant0.966$
[53]	189	177.3	$4.35\pm0.17\pm0.09$	4.66 ± 0.03	643	82.1	$x_T>0.05$	$\leqslant0.966$

[a]Estimated from the Monte Carlo cross sections and the expected numbers of events.
[b]The STIC efficiency varies between 74% and 27% over the angular region used in the analysis.
[c]Calculated from the expected number of events as predicted by the KORALZ event generator.

mated the Monte Carlo cross sections from the published numbers of events expected as predicted by the KORALZ event generator. The results agree well with our estimates.

The 90% C.L. implied by LEP-2 data read

$$-8.2\times10^{-32}\ \mathrm{cm}^2\leqslant\langle r_A^2(\nu_\tau)\rangle\leqslant9.9\times10^{-32}\ \mathrm{cm}^2 \tag{3.18}$$

for the Majorana case, and

$$-5.6\times10^{-32}\ \mathrm{cm}^2\leqslant\langle r_{V,A}^2(\nu_\tau)\rangle\leqslant6.2\times10^{-32}\ \mathrm{cm}^2 \tag{3.19}$$

for a Dirac ν_τ.

These limits are about a factor of 4 stronger than the limits derived in [29] from the SNO and Super-Kamiokande observations and than the limits obtained in [30] from just the TRISTAN data. In Fig. 1 we depict the 90% C.L. on $\langle r_V^2(\nu_\tau)\rangle$ and $\langle r_A^2(\nu_\tau)\rangle$ for the Dirac case as derived from the LEP-2 data. The picture shows the absence of any strong correlation between $\langle r_V^2(\nu_\tau)\rangle$ and $\langle r_A^2(\nu_\tau)\rangle$. We stress that the possibility of bounding simultaneously the vector and axial vector charge radii stems from the fact that in e^+e^- annihilation right-handed neutrinos can also be produced, and they couple to the photon through a combination of $\langle r_V^2\rangle$ and $\langle r_A^2\rangle$ that is orthogonal to the one that couples the left-handed neutrinos. In contrast, neutrino scattering experiments do not involve the right-handed neutrinos, and therefore can only bound the combination $\langle r_V^2\rangle+\langle r_A^2\rangle$.

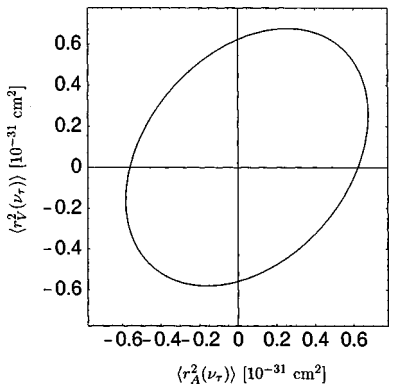

FIG. 1. Combined limits on $\langle r_V^2(\nu_\tau)\rangle$ and $\langle r_A^2(\nu_\tau)\rangle$ for Dirac tau neutrinos derived from LEP-2 data. The plot shows the $\chi^2_{\rm min}+2.71$ contour, corresponding to 90% C.L.

Before concluding this section, we should mention that independent limits could also be derived from the DONUT experiment, through an analysis similar to the one presented in [54], and that yielded limits on the ν_τ magnetic moment. We have estimated that the constraints from DONUT would be at least one order of magnitude worse than the limits obtained from LEP; however, it should be remarked that these limits would be inferred directly from the absence of anomalous interactions for a neutrino beam with an identified ν_τ component [55].

IV. LIMITS ON ν_μ VECTOR AND AXIAL VECTOR CHARGE RADIUS

The NuTeV Collaboration has recently published a value of $\sin^2\theta_W$ measured from the ratio of neutral current to charged current in deep inelastic ν_μ-nucleon scattering [56]. Their result reads

$$\sin^2\theta_W^{(\nu)} = 0.2277 \pm 0.0013 \pm 0.0009 \tag{4.1}$$

where the first error is statistical and the second error is systematic. In order to derive limits on neutrino electromagnetic properties one should compare the results obtained in neutrino experiments to a value of $\sin^2\theta_W$ determined from experiments that do not involve neutrinos. Currently, the most precise value of $\sin^2\theta_W$ from non-neutrino experiments comes from measurements at the Z pole and from direct measurements of the W mass [57]. In our numerical calculations we will use the value for $\sin^2\theta_W$ obtained from a global fit to electroweak measurements without neutrino-nucleon scattering data, as reported in [56,58]:

$$\sin^2\theta_W = 0.2227 \pm 0.00037. \tag{4.2}$$

The effect of a nonvanishing charge radius can be taken into account through the replacement $g_V \to g_V - \delta$ in the formulas for ν_μ-nucleon and ν_μ-electron scattering [59], where δ is given in Eq. (3.11). Since there are no right-handed neutrinos involved, there is no effect proportional to δ' and therefore only $\delta \propto \langle r_V^2(\nu_\mu)\rangle + \langle r_A^2(\nu_\mu)\rangle$ can be constrained. Upper and lower limits can be directly derived by comparing $\sin^2\theta_W^{(\nu)}$ with the quoted value of $\sin^2\theta_W$ from non-neutrino experiments. Since the results for neutrino experiments and the measurements at the Z pole are not consistent at the 1σ level, in the following equations (4.3)–(4.5) we will (conservatively) combine the errors by adding them linearly.[5]

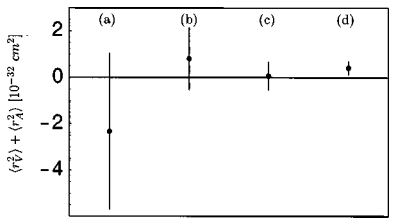

FIG. 2. 90 % C.L. on $(\langle r_V^2\rangle + \langle r_A^2\rangle)$ for the muon neutrino derived from (a) E734 at BNL [28], (b) CHARM II [27], (c) the CCFR experiment [60], and (d) the NuTeV result [56].

From the NuTeV result (4.1) we obtain the 90% C.L. upper limit

$$\langle r_V^2(\nu_\mu)\rangle + \langle r_A^2(\nu_\mu)\rangle \leq 7.1\times 10^{-33}\ \text{cm}^2; \tag{4.3}$$

however, since Eq. (4.1) hints at a nonvanishing value of δ (see Fig. 2), no lower limit is obtained from this measurement. A reanalysis of the E734 data on ν_μ-e and $\overline{\nu}_\mu$-e scattering [28] yields the 90% C.L.:

$$-5.7\times 10^{-32}\ \text{cm}^2 \leq \langle r_V^2(\nu_\mu)\rangle + \langle r_A^2(\nu_\mu)\rangle \leq 1.1\times 10^{-32}\ \text{cm}^2. \tag{4.4}$$

Note that in Ref. [28] the E734 Collaboration is quoting a lower limit about 3.6 times and an upper limit about 7.5 times tighter than the ones given in Eq. (4.4). This is for various reasons: First of all, as was pointed out in [61], in [28] an inconsistent value for G_F was used that resulted in bounds stronger by approximately a factor of $\sqrt{2}$. In addition, the errors were combined quadratically, which, due to the large negative trend in their data, resulted in a much stronger upper bound on $\langle r_V^2(\nu_\mu)\rangle + \langle r_A^2(\nu_\mu)\rangle$ than the one quoted here. Finally, our value of δ is defined through the shift $g_V \to g_V - \delta$ of the SM vector coupling, consistently, for example, with the notation of [59], while the convention used by the E734 Collaboration [28] as well as by CHARM II [27] define δ as a shift in $\sin^2\theta_W$. This implies that our limits are larger by an additional factor of 2 with respect to the results published by these two collaborations.

From the CHARM II neutrino-electron scattering data [27] we obtain at 90% C.L.:

$$-0.52\times 10^{-32}\ \text{cm}^2 \leq \langle r_V^2(\nu_\mu)\rangle + \langle r_A^2(\nu_\mu)\rangle \leq 2.2\times 10^{-32}\ \text{cm}^2. \tag{4.5}$$

These limits differ from the numbers published by the CHARM II Collaboration [27] not only because of the mentioned factor of 2 in the definition of δ, but also because the

[5]Except for the CCFR data, which are consistent with the SM precision fits.

present value of $\sin^2\theta_W$ [57] is smaller than the one used in 1995 in the CHARM II analysis.

From the data published by the CCFR Collaboration [60] one can deduce

$$-0.53\times10^{-32}\ \text{cm}^2 \leq \langle r_V^2(\nu_\mu)\rangle + \langle r_A^2(\nu_\mu)\rangle \leq 0.68\times10^{-32}\ \text{cm}^2. \quad (4.6)$$

The four limits discussed above are represented in Fig. 2, which makes apparent the level of precision of the NuTeV result. By combining the upper limit from CCFR [Eq. (4.6)] and the lower limit from CHARM II [Eq. (4.5)] we finally obtain

$$-5.2\times10^{-33}\ \text{cm}^2 \leq \langle r_V^2(\nu_\mu)\rangle + \langle r_A^2(\nu_\mu)\rangle \leq 6.8\times10^{-33}\ \text{cm}^2. \quad (4.7)$$

It is well known that the NuTeV result shows a sizable deviation from the SM predictions [56], and as a consequence it also appears to be inconsistent (at the 90% C.L.) with $\delta=0$. In fact, strictly speaking, their result $\langle r_V^2(\nu_\mu)\rangle + \langle r_A^2(\nu_\mu)\rangle = (4.20\pm1.64)\times10^{-33}\ \text{cm}^2$ (1σ error) could be interpreted as a measurement of $\langle r_V^2(\nu_\mu)\rangle + \langle r_A^2(\nu_\mu)\rangle$, which becomes consistent with zero only at approximately 2.5 standard deviations. However, while the quoted value is not in conflict with other experimental limits, we believe that it would be not easy to construct a model that could generate a neutrino charge radius of the required size, without conflicting with other high precision electroweak measurements. A comprehensive analysis of different possible interpretations of the NuTeV anomaly can be found in [62].

V. CONCLUSIONS

This work stems from the observation that if neutrinos are Majorana particles their axial charge radius $\langle r_A^2\rangle$, which is the only permitted flavor diagonal electromagnetic form factor, cannot be constrained through astrophysical or cosmological observations. In Sec. II we discussed in some detail how it is not possible to derive useful constraints from nucleosynthesis and from measurements of primordial helium abundance. We concluded that in order to constrain $\langle r_A^2\rangle$ we can rely only on the analysis of the results of terrestrial experiments.

In Sec. III we presented a comprehensive analysis of the available off Z-resonance data for the process $e^+e^-\to\nu\bar{\nu}\gamma$. We used these data to derive limits for the axial vector charge radius of the τ neutrino, as well as the combined limits on the vector and axial vector charge radii in the case of a Dirac ν_τ. These limits are largely dominated by the high statistics LEP-2 data collected above the W^+W^- production threshold.

We also analyzed the bounds that can be derived for the muon neutrino from an analysis of neutrino scattering experiments. We obtained the most stringent limits by combining the CCFR ν_μ-nucleon scattering and the CHARM II ν_μ-electron scattering results. No new limits were obtained for the electron-neutrino orientation; however, new experiments dedicated to the detailed study of electron-(anti)neutrino interactions with matter, such as, for example, the MUNU experiment at the Bugey nuclear reactor [63], should be able to improve existing limits by about one order of magnitude.

ACKNOWLEDGMENTS

This work was supported in part by COLCIENCIAS in Colombia and by CSIC in Spain through a joint program for international scientific cooperation, and in part by the Spanish Grant BFM2002-00345 and by the European Commission RTN Network HPRN-CT-2000-00148. M.H. is supported by a Spanish MCyT Ramon y Cajal contract.

[1] Super-Kamiokande Collaboration, T. Toshito, hep-ex/0105023.
[2] Super-Kamiokande Collaboration, S. Fukuda *et al.*, Phys. Rev. Lett. **85**, 3999 (2000).
[3] Super-Kamiokande Collaboration, S. Fukuda *et al.*, Phys. Rev. Lett. **86**, 5651 (2001).
[4] SNO Collaboration, Q.R. Ahmad *et al.*, Phys. Rev. Lett. **89**, 011301 (2002).
[5] A.D. Dolgov, Phys. Rep. **370**, 333 (2002).
[6] R.N. Mohapatra and P.B. Pal, *Massive Neutrinos in Physics and Astrophysics*, 2nd ed. (World Scientific, Singapore, 1998).
[7] G.G. Raffelt, *Stars as Laboratories for Fundamental Physics: The Astrophysics of Neutrinos, Axions, and Other Weakly Interacting Particles* (Chicago University Press, Chicago, 1996).
[8] E.K. Akhmedov and J. Pulido, Phys. Lett. B **529**, 193 (2002).
[9] J. Pulido, Astropart. Phys. **18**, 173 (2002).
[10] O.G. Miranda, C. Pena-Garay, T.I. Rashba, V.B. Semikoz, and J.W. Valle, Phys. Lett. B **521**, 299 (2001); Nucl. Phys. **B595**, 360 (2001).
[11] E.K. Akhmedov and J. Pulido, Phys. Lett. B **485**, 178 (2000).
[12] J. Pulido and E.K. Akhmedov, Astropart. Phys. **13**, 227 (2000).
[13] M.M. Guzzo and H. Nunokawa, Astropart. Phys. **12**, 87 (1999).
[14] J.F. Nieves, Phys. Rev. D **26**, 3152 (1982).
[15] R.E. Shrock, Nucl. Phys. **B206**, 359 (1982).
[16] See, for example, G. Degrassi, A. Sirlin, and W.J. Marciano, Phys. Rev. D **39**, 287 (1989); M.J. Musolf and B.R. Holstein, *ibid.* **43**, 2956 (1991). A complete list can be found in [17].
[17] J. Bernabeu, L.G. Cabral-Rosetti, J. Papavassiliou, and J. Vidal, Phys. Rev. D **62**, 113012 (2000).
[18] J. Bernabeu, J. Papavassiliou, and J. Vidal, Phys. Rev. Lett. **89**, 101802 (2002).
[19] L.G. Cabral-Rosetti, M. Moreno, and A. Rosado, hep-ph/0206083.
[20] J. Bernabeu, J. Papavassiliou, and J. Vidal, hep-ph/0210055.
[21] B. Kayser, Phys. Rev. D **26**, 1662 (1982).
[22] V.M. Dubovik and V.E. Kuznetsov, Int. J. Mod. Phys. A **13**, 5257 (1998).
[23] G.G. Raffelt, Phys. Rep. **320**, 319 (1999).

[24] J.A. Grifols and E. Masso, Phys. Rev. D **40**, 3819 (1989).
[25] J.A. Grifols and E. Masso, Mod. Phys. Lett. A **2**, 205 (1987).
[26] R.C. Allen *et al.*, Phys. Rev. D **47**, 11 (1993).
[27] CHARM-II Collaboration, P. Vilain *et al.*, Phys. Lett. B **345**, 115 (1995).
[28] E734 Collaboration, L.A. Ahrens *et al.*, Phys. Rev. D **41**, 3297 (1990).
[29] A.S. Joshipura and S. Mohanty, hep-ph/0108018.
[30] N. Tanimoto, I. Nakano, and M. Sakuda, Phys. Lett. B **478**, 1 (2000).
[31] Y. Declais *et al.*, Nucl. Phys. **B434**, 503 (1995).
[32] D.A. Dicus, E.W. Kolb, A.M. Gleeson, E.C. Sudarshan, V.L. Teplitz, and M.S. Turner, Phys. Rev. D **26**, 2694 (1982).
[33] E.W. Kolb and M.S. Turner, *The Early Universe*, Frontiers in Physics Vol. 69 (Addison-Wesley, Redwood City, CA, 1990).
[34] R.E. Lopez and M.S. Turner, Phys. Rev. D **59**, 103502 (1999).
[35] A.D. Dolgov, Nucl. Phys. B (Proc. Suppl.) **110**, 137 (2002).
[36] K.J. Gaemers, R. Gastmans, and F.M. Renard, Phys. Rev. D **19**, 1605 (1979).
[37] D. Bardin, S. Jadach, T. Riemann, and Z. Was, Eur. Phys. J. C **24**, 373 (2002).
[38] AMY Collaboration, Y. Sugimoto *et al.*, Phys. Lett. B **369**, 86 (1996).
[39] TOPAZ Collaboration, T. Abe *et al.*, Phys. Lett. B **361**, 199 (1995).
[40] VENUS Collaboration, N. Hosoda *et al.*, Phys. Lett. B **331**, 211 (1994).
[41] ALEPH Collaboration, D. Buskulic *et al.*, Phys. Lett. B **384**, 333 (1996).
[42] DELPHI Collaboration, W. Adam *et al.*, Phys. Lett. B **380**, 471 (1996).
[43] OPAL Collaboration, G. Alexander *et al.*, Phys. Lett. B **377**, 222 (1996).
[44] OPAL Collaboration, K. Ackerstaff *et al.*, Eur. Phys. J. C **2**, 607 (1998).
[45] OPAL Collaboration, G. Abbiendi *et al.*, Eur. Phys. J. C **8**, 23 (1999).
[46] ALEPH Collaboration, R. Barate *et al.*, Phys. Lett. B **420**, 127 (1998).
[47] ALEPH Collaboration, R. Barate *et al.*, Phys. Lett. B **429**, 201 (1998).
[48] ALEPH Collaboration, A. Heister *et al.*, Report No. CERN-EP-2002-033.
[49] DELPHI Collaboration, P. Abreu *et al.*, Eur. Phys. J. C **17**, 53 (2000).
[50] L3 Collaboration, M. Acciarri *et al.*, Phys. Lett. B **415**, 299 (1997).
[51] L3 Collaboration, M. Acciarri *et al.*, Phys. Lett. B **444**, 503 (1998).
[52] L3 Collaboration, M. Acciarri *et al.*, Phys. Lett. B **470**, 268 (1999).
[53] OPAL Collaboration, G. Abbiendi *et al.*, Eur. Phys. J. C **18**, 253 (2000).
[54] DONUT Collaboration, R. Schwienhorst *et al.*, Phys. Lett. B **513**, 23 (2001).
[55] DONUT Collaboration, K. Kodama *et al.*, Phys. Lett. B **504**, 218 (2001).
[56] NuTeV Collaboration, G.P. Zeller *et al.*, Phys. Rev. Lett. **88**, 091802 (2002).
[57] Particle Data Group, K. Hagiwara *et al.*, Phys. Rev. D **66**, 010001 (2002).
[58] NuTeV Collaboration, G.P. Zeller, hep-ex/0207037.
[59] P. Vogel and J. Engel, Phys. Rev. D **39**, 3378 (1989).
[60] CCFR Collaboration, K.S. McFarland *et al.*, Eur. Phys. J. C **1**, 509 (1998).
[61] R.C. Allen *et al.*, Phys. Rev. D **43**, R1 (1991).
[62] S. Davidson, S. Forte, P. Gambino, N. Rius, and A. Strumia, J. High Energy Phys. **02**, 037 (2002).
[63] MUNU Collaboration, C. Broggini, Nucl. Phys. B (Proc. Suppl.) **110**, 398 (2002).